Electron paramagnetic resonance and electron–nuclear double resonance characterization of radicals in photopolymerized multifunctional methacrylates

Cesare Oliva,* Elena Selli, Silvia Di Blas and Giorgio Termignone
Dipartimento di Chimica Fisica ed Elettrochimica and Centro C. N. R., Università di Milano, via Golgi 19, I 20133 Milano, Italy

Propagation radicals generated during the photopolymerization and photo-cross-linking of a trimethacrylate and a vinylmethacrylate monomer have been characterized by EPR and ENDOR spectroscopy at different temperatures. Also, radical decay has been investigated at 363–423 K. The EPR spectral shape reflects a fast exchange process between two radical conformations and is sensitive to the mobility of the polymeric structure surrounding radicals. ENDOR spectra show ^{1}H-matrix lines and a band around 45 MHz, which has been attributed to the interaction of the unpaired electron with the hydrogen nuclei of a freely rotating methyl group. Radical decay and dynamic phenomena involving radicals have been interpreted in the light of a dispersive kinetic model, which allows the evaluation of useful parameters for polymer characterization.

Introduction

Electron paramagnetic resonance (EPR) spectroscopy is the best method to determine the structure and concentration of radicals propagating in liquids[1] or solids as well as those trapped in the solid phase during radical polymerizations,[2] and also the only one which allows the evaluation of kinetic coefficients in glassy polymers, such as those produced by photoinduced polymerization of multifunctional acrylic, methacrylic and vinylic monomers. With these monomeric systems, the reaction does not proceed according to the classical polymerization mechanism.[3] In fact, with increasing conversion of double bonds, the formation of a network, due to the presence of more than one reactive group in each monomeric unit, and the subsequent early vitrification progressively inhibit the diffusion of the reactive groups towards chain-propagating free radicals. Therefore, radicals remain occluded in the polymer network, chain transfer gradually gains in importance, and all rate coefficients become dependent on conversion.[4–6]

However, in the application of EPR spectroscopy to polymerization kinetic studies some problems have been noted,[7] partly due to the difficulty with which correct quantitative evaluations can be obtained for radical concentration. Moreover, the existence of inhomogeneities in the polymeric structure, due to the formation of microgel particles in the pre-gel stage, has been evidenced in the photopolymerization of multifunctional monomers by different experimental techniques.[8] The contemporary presence of different types of radicals and the fact that their reactivity might be modified by the polymeric environment further complicate the system under study.[9] In particular, this is the situation observed in photopolymerized multiacrylate monomers.[10–13] Anyway, the dependence of radical reactivity on the polymeric surrounding is not just a source of complication, but it can also be envisaged as a tool for the characterization of the polymeric structure. In fact, trapped radicals give EPR signals with spectral shapes which can be sensitive to the mobility of the polymeric environment. Valuable information can also be obtained from the rate law of radical decay in photopolymerized samples kept at temperatures above ambient, through the measurement of the decay rate of different EPR signals. Also, electron–nuclear double resonance (ENDOR) analysis of trapped radicals contributes to the elucidation of the characteristics of the polymer structure: in photopolymerized multiacrylate monomers ^{1}H-matrix lines, typical of the solid state, were observed, due to hydrogen nuclei interacting with the unpaired electron spin.[10,11]

Our investigations have recently been extended to radicals generated during the photopolymerization of other multifunctional monomeric systems, and in particular to methacrylates. In a preceding paper a model has been proposed to account for the EPR spectra obtained from radicals produced during the photopolymerization of a dimethacrylate monomer, ethylene glycol dimethacrylate (2-methylprop-2-enoic acid ethane-1,2-diyl ester) (DMA).[14] By this model, the nine-line EPR spectrum generated by the propagating free radical (see structure **1**) was

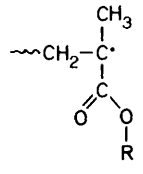

1

interpreted as being due to the interaction of the unpaired electron with the freely rotating methyl group and with the β-methylene group, which undergoes a fast dynamic exchange between two conformations of the growing polymeric chain. All couplings were there considered as isotropic.

In the present work we report the EPR and ENDOR characterization of radicals trapped during the photoinduced polymerization of a trimethacrylate monomer (TMA), which leads to a highly cross-linked polymer structure, and of a vinylmethacrylate monomer (VMA), a difunctional monomer carrying different reactive groups. Moreover, radical decay in post-irradiation heat treatment and dynamic phenomena involving radicals have been interpreted in the light of a dispersive kinetic model.

Experimental

Materials and sample preparation

Monomers and photoinitiator were commercial products. Trimethylolpropane trimethacrylate (TMA) {$[H_2C{=}C(CH_3)\text{-}CO_2CH_2]_3CC_2H_5$, 2-methylprop-2-enoic acid 2-ethyl-2-{[(2-methyl-1-oxoprop-2-enyl)oxy]methyl}propane-1,3-diyl ester} was purchased from Aldrich, Germany. Vinyl methacrylate

(VMA) [$H_2C{=}C(CH_3)CO_2CH{=}CH_2$, 2-methylprop-2-enoic acid ethenyl ester] was a Lancaster, UK, product. They were washed with aq. sodium hydroxide to remove inhibitor (hydroquinone monomethyl ether) and then several times with saturated aq. NaCl. They were successively dried over anhydrous sodium sulfate and molecular sieves 4 Å (Union Carbide, USA) and then stored at 4 °C in the dark. The photoinitiator, 2,2-dimethoxy-1,2-diphenylethanone, from BASF, Germany, was used as received.

The monomers, mixed with 1.0 wt.% of photoinitiator, were sealed under vacuum in a quartz tube and then irradiated with UV–VIS light outside the spectrometer cavity. The previously described apparatus and experimental standard procedure were employed.[10,11] According to Raman spectroscopic analysis,[14,15] at the end of irradiation the degree of double-bond conversion was ~60% in photopolymerized TMA and ~50% in photopolymerized VMA.

EPR and ENDOR spectroscopy and fitting procedure

EPR and ENDOR spectra of pre-irradiated samples were recorded at different temperatures on a Bruker ESP 300 EPR/ENDOR spectrometer, under the same conditions as already described.[14] The employed microwave frequency was 9.39 GHz, its power was 0.2 mW, and the 100 KHz modulation amplitude was 0.5 G. EPR digitized spectra were fitted according to the already reported non-linear least-squares fitting procedure,[13,16] yielding width, hyperfine splitting, *g*-factor, spectral area of each overlapping EPR pattern, and also parameters of linewidth variation resulting from dynamic processes involving radicals. The statistical error affecting each parameter was also obtained.

The radical concentration, assumed to be proportional to the numerical integrated area of the corresponding EPR pattern, was roughly estimated through a calibration of the instrument by means of a Varian strong pitch.

Results

EPR spectra at room temperature

The EPR spectra obtained at room temperature from photopolymerized samples of both trimethacrylate monomer TMA and vinylmethacrylate monomer VMA consist of a nine-line EPR pattern, typical of methacrylate propagating radicals (structure **1**). Very good fittings of the experimental spectra (see Fig. 1) were obtained by attributing the nine lines to three equivalent hydrogen atoms with hyperfine coupling constant (hfcc) a_{3H} = 2.22 ± 0.02 mT for pre-irradiated TMA and a_{3H} = 2.25 ± 0.01 mT for pre-irradiated VMA, and to two equivalent hydrogen atoms with hfcc a_{2H} = 1.17 ± 0.02 mT and 1.22 ± 0.01 mT, respectively, for the two pre-irradiated systems. The intrinsic linewidth of the EPR patterns is ΔW_0 = 0.77 ± 0.01 mT and 0.70 ± 0.01 mT in the two cases. An additional broadening contribution ΔW_{exch} = 0.57 ± 0.01 mT and 0.51 ± 0.02 mT is measured for the central line of the hydrogen multiplet characterized by a_{2H} of pre-irradiated TMA and VMA, respectively.

EPR spectra at different temperatures

The spectral shape does not change with temperature in the range 153–373 K, while major changes occur at temperatures above 373 K for both pre-irradiated systems (see, for example, Fig. 2 for TMA). At such high temperatures much better fittings of the experimental spectra can be obtained by assuming that a single-line pattern, with the same *g*-value, overlaps the nine-line signal. The ratio of the concentration of radicals giving the single-line pattern over that of the species giving the nine-line pattern increases with temperature, being 0.5/100 for TMA at 383 K and nearly 10 times higher for VMA at the same temperature, while it attains the same value of 50/100 in both systems at 443 K.

The increase in concentration of the single-line carrier is accompanied by an increase in both line intensity and linewidth of this EPR pattern. At 383 K, the last parameter is 0.28 ± 0.03

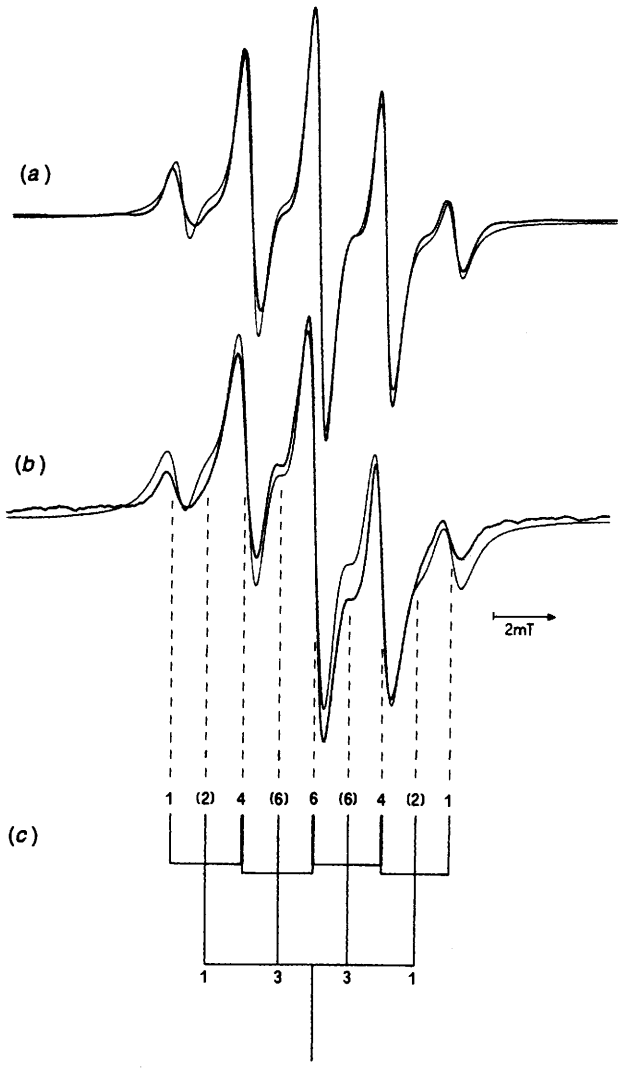

Fig. 1 Experimental (noisy trace) and computer-simulated spectrum of pre-irradiated (*a*) TMA and (*b*) VMA at room temperature and (*c*) interpretation scheme. Thick lines are due to the overlapping of lines unaffected by the motional broadening; the degeneration of the motional broadened lines is reported in parentheses.

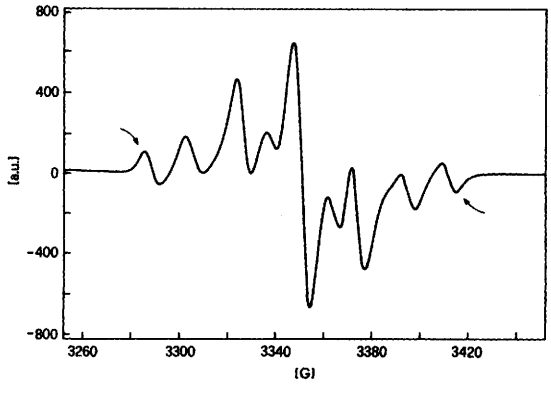

Fig. 2 EPR spectrum of pre-irradiated TMA at 443 K. The new EPR lines are indicated by arrows.

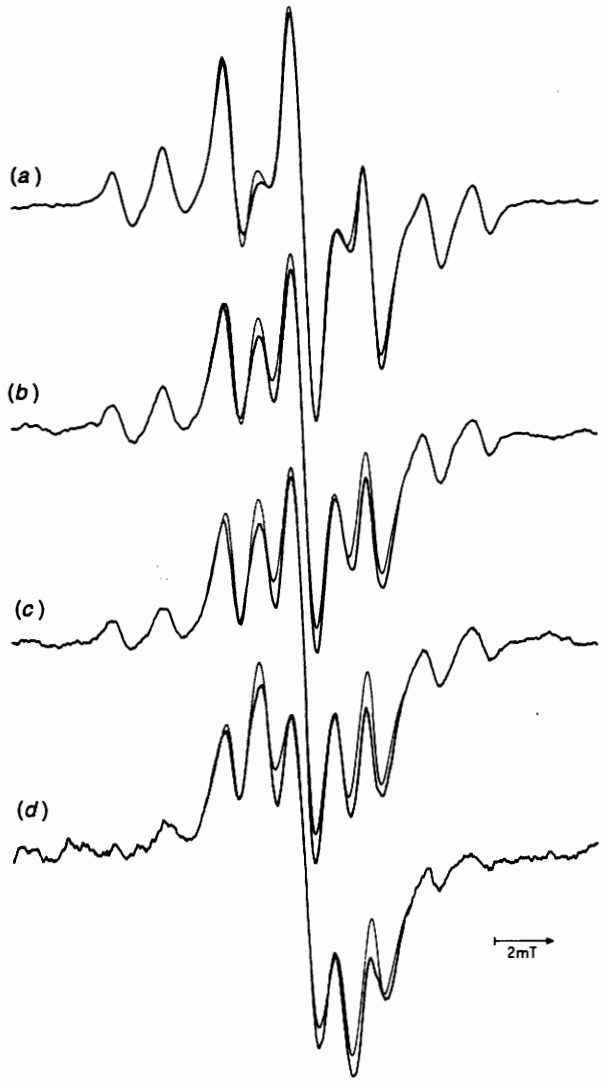

Fig. 3 EPR spectra of pre-irradiated TMA at various times during radical decay at 423 K (noisy trace) and least-squares fittings of their central parts. Maximum spectral intensity was normalized. (*a*) 0, (*b*) 30, (*c*) 60, (*d*) 310 min.

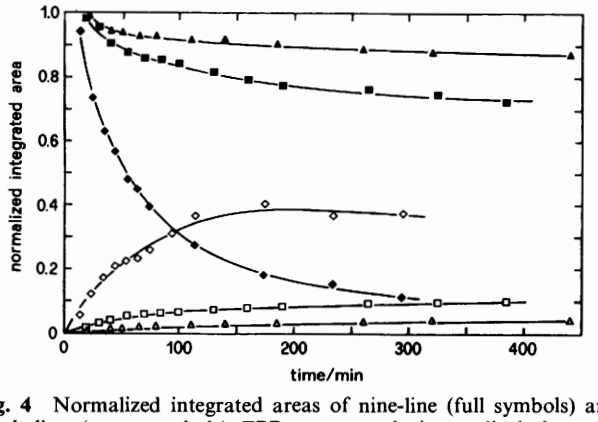

Fig. 4 Normalized integrated areas of nine-line (full symbols) and single-line (open symbols) EPR patterns during radical decay at different temperatures in pre-irradiated TMA. (▲, △) 363 K, (■, □) 393 K, (◆, ◇) 423 K.

mT (TMA) and 0.48 ± 0.02 mT (VMA), while at 443 K it attains the values of 1.95 ± 0.06 mT (TMA) and 1.54 ± 0.04 mT (VMA). Also, a variation of ΔW_{exch} is seen to occur with temperature. In fact ΔW_{exch} = 0.54 ± 0.01 mT (TMA)

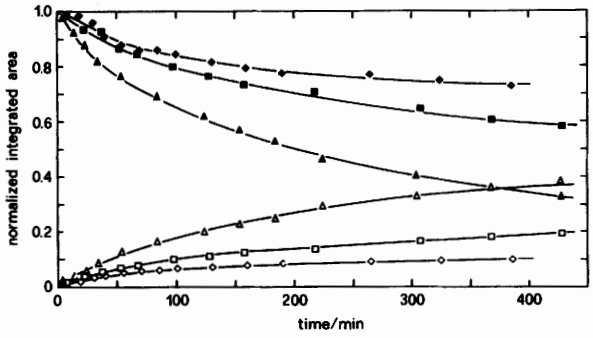

Fig. 5 Normalized integrated areas of nine-line (full symbols) and single-line (open symbols) EPR patterns during radical decay at 393 K in photopolymerized methacrylate systems. (◆, ◇) TMA, (▲, △) DMA and (■, □) a 50/50 wt.% mixture of the two monomers.

and 0.511 ± 0.009 mT (VMA) at 383 K, while ΔW_{exch} = 0.37 ± 0.02 mT (TMA) and 0.41 ± 0.01 mT (VMA) at 443 K.

Moreover, two new lines appear on both sides of the EPR spectrum of pre-irradiated TMA at temperatures above 383 K (Fig. 2), which do not disappear after cooling the sample back to room temperature. These two features are not observed with photopolymerized VMA.

EPR spectra during radical decay

The EPR spectral shape undergoes marked modifications during radical decay kinetic runs in the range 363–423 K, showing the same trend for both photopolymerized systems. An example of this behaviour is illustrated in Fig. 3. According to the results of the fitting procedure, the integrated area of the single-line spectrum continuously increases during radical decay, while the integrated area of the whole EPR pattern decreases at different rates, depending on temperature. The decay with time of the integrated area of the nine-line EPR spectrum of photopolymerized TMA and the increase of the integrated area of the single line for the same system are compared in Fig. 4 for three temperatures.

The trend shown for radical decay at 393 K in this system is also compared in Fig. 5 with analogous results already reported by us[14] for pre-irradiated DMA and with the behaviour observed in the present investigation for radical decay in a photopolymerized system obtained by irradiating a 50/50 wt.% mixture of the two monomers. The nine-line pattern decays more slowly and at the same time the concentration of the single line carrier increases more slowly in photopolymerized TMA with respect to DMA, while the pre-irradiated mixture of the two monomers shows an intermediate behaviour.

Note also that ΔW_{exch} changes with time during radical decay, decreasing in all cases. This trend will be discussed below.

ENDOR spectra

^{1}H-Matrix ENDOR spectra of radicals produced in photopolymerized multifunctional methacrylate systems (DMA, TMA and VMA) are detectable at room temperature. However, at low temperature these patterns are more intense and in the cases of DMA and TMA they also resolve into two bands of different width (Fig. 6). A second feature around 45 MHz also adds to the matrix band at low temperature, the intensity of which is in the order TMA > DMA > VMA at 120 K (Fig. 7). At room temperature this band is twice as intense as that at 120 K for TMA, whilst it is unchanged with DMA, and completely disappears in the case of VMA. In all cases, anyway, this EPR feature irreversibly disappears on heating of the sample at 393 K for 1 h.

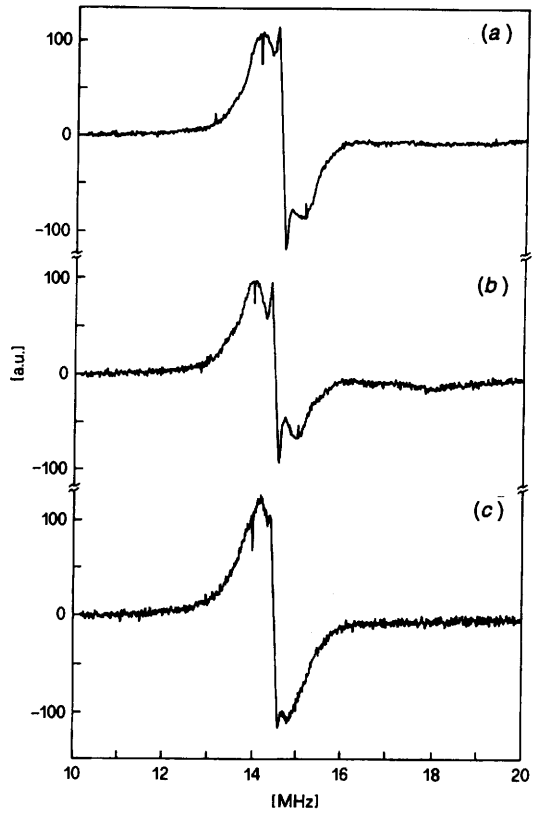

Fig. 6 ^{1}H-matrix ENDOR spectra of photopolymerized (*a*) TMA, (*b*) DMA and (*c*) VMA at 120 K

Discussion

The nature of trapped radicals

Both photopolymerized monomers give a nine-line EPR spectrum, thus indicating that in the case of pre-irradiated vinyl methacrylate the most stable species detectable by EPR is the propagation radical of the methacrylate group (structure 1), although polymerization can take place also on the vinyl group. Propagating radicals obtained from vinyl acetate have been reported elsewhere and show a completely different EPR spectrum.[17]

The model adopted for the interpretation of the EPR spectra obtained in this work with photopolymerized TMA and VMA is analogous to that already adopted by us in a previous work[14] concerning photopolymerized DMA. Thus, the nine-line spectrum results from the interaction of the unpaired electron of the propagation radical (structure 1) with the three completely equivalent hydrogen atoms of the methyl group and with the two β-methylene hydrogens, which undergo a fast chemical exchange between two different conformations. The single-line spectrum also originates from the same propagation radicals. The lack of hyperfine splitting is a consequence of a spin–spin interaction between radicals trapped within a rigid matrix. This phenomenon is negligible at room temperature, but increases in importance at higher temperatures, due to further polymerization and cross-linking of the samples leading to an increase in rigidity of the medium.

This is in agreement with that reported elsewhere[10–13] in the case of radicals produced in the photopolymerization of multifunctional acrylates and is further confirmed by the analysis of the ^{1}H-matrix ENDOR spectra (Figs. 6 and 7). In fact, the last are typical of solid-state samples. In the framework of the point dipole approximation, it is also possible to evaluate the distance *r* between the unpaired electron and the shell of the nearest neighbour interacting protons, through eqn. (1)[18]

Table 1 ^{1}H-Matrix ENDOR results for methacrylic monomers pre-irradiated in the presence of 1.0 wt.% photoinitiator. δ is peak-to-peak linewidth (maximum dipolar constant value) and *r* is the distance between the unpaired electron and the surrounding shell(s) of protons

Monomer	*T*/K	δ/MHz	*r*/Å
TMA	295	0.84	4.6
TMA	120	0.97–0.21	4.3–7.2
DMA	295	0.91	4.4
DMA	120	0.89–0.19	4.8–7.5
VMA	295	0.63	5.0
VMA	120	0.59–0.19	5.1–7.5

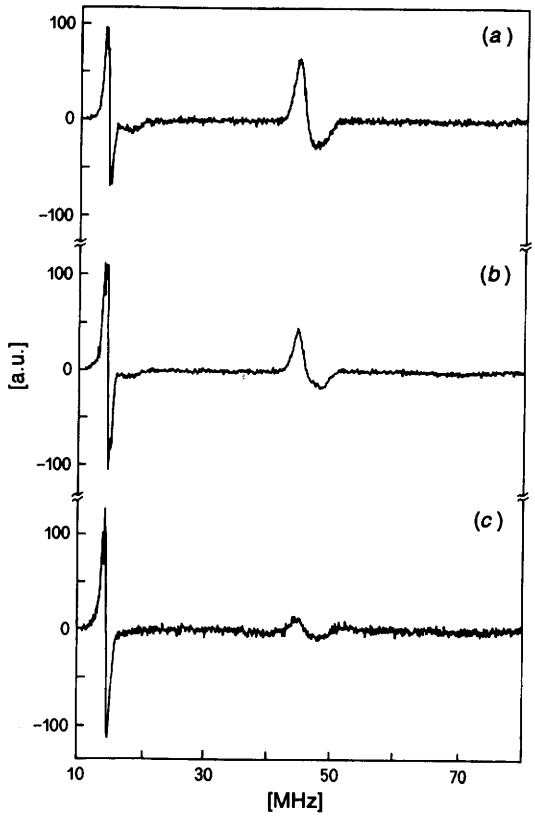

Fig. 7 ENDOR spectra of photopolymerized (*a*) TMA, (*b*) DMA and (*c*) VMA at 120 K

$$\delta = 80/r^3 \quad (1)$$

where *r* is in Å (10 Å = 1 nm) and δ is the dipolar constant in MHz. δ is always less than the experimental width of the matrix ENDOR line. In this way the electron–proton distances reported in Table 1 have been evaluated.

The decrease of ΔW_{exch} with increasing temperature evidences the increase in the exchange speed between the two possible radical conformations, corresponding, as for photopolymerized DMA, to two orientations of the CH_2 group with respect to the C_α–C_β bond.[14] The exchange time t_{exch}, evaluated from the ΔW_{exch} in a standard way,[19] decreases with increasing molar fraction $x(S^\bullet)$ of the 'solid' species $S^\bullet$, characterized by the single-line EPR feature, as shown in Fig. 8 for photopolymerized DMA and TMA. Each system shows a typical trend of the t_{exch} *vs.* $x(S^\bullet)$ plot, which is independent of the radical decay temperature, but should be related to the characteristics of the polymerized structure. For $x(S^\bullet)$-values in the range $0.1 < x(S^\bullet) < 0.8$, t_{exch} is shorter for TMA than for DMA. However, during radical decay the same $x(S^\bullet)$-value is reached later in photopolymerized TMA than in DMA (*cf.* Fig. 5).

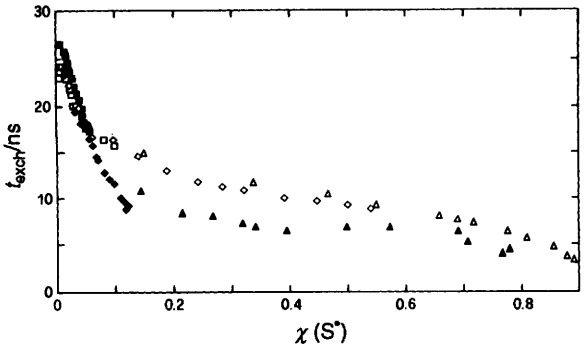

Fig. 8 Exchange time between radical conformations $R_1^{\bullet}$ and $R_2^{\bullet}$ *vs.* mole fraction x(S•). Data have been calculated from the EPR spectra recorded at (■, □) 363 K, (◆, ◇) 393 K and (▲, △) 423 K during radical decay kinetic runs in TMA (full symbols) and DMA (open symbols, taken from ref. 14) photopolymerized in the presence of 1.0 wt.% photoinitiator.

The behaviour shown in Fig. 8 indicates that the exchange between the two radical conformations $R_1^{\bullet}$ and $R_2^{\bullet}$ does not involve just the more 'fluid' species R• characterized by the nine-line EPR pattern, but is an intermolecular phenomenon, involving also S• species, being represented by eqn. (2).

$$R_1^{\bullet} + S^{\bullet} \rightleftharpoons R_2^{\bullet} + S^{\bullet} \qquad (2)$$

The ENDOR band observed in the region around 45 MHz (Fig. 7) can be safely attributed to the hydrogen nuclei belonging to the rotating methyl group. It has been reported[20,21] that this dynamic phenomenon modulates the hfcc of the hydrogen nuclei, becoming a very effective source of relaxation of the electronic level population through the flip-flop ($\Delta M_S + \Delta M_I = 0$) transition. From the data reported in the literature for irradiated Li-lactate[21] and (−)-alanine[20] one can easily calculate, for example, that τ, the average time between consecutive jumps of the methyl group, is 0.4 ps and 4×10^4 ps, in the two cases respectively. These results indicate that the rotation rate can assume values over a very large interval.

On the other hand, the ENDOR line-intensity enhancement factor E calculated in this framework depends on τ, being given by eqn. (3), where WE is the transition probability of the

$$E \div \frac{1}{WE} \frac{\tau}{(1 + \omega^2\tau^2)} \qquad (3)$$

electron spin transition. Very slow ($\tau \rightarrow \infty$) and very fast ($\tau \rightarrow 0$) rotations are inefficient in producing ENDOR enhancement, whilst a maximum enhancement is obtained when the rotation rate τ^{-1} is identical with the radio frequency ω employed to detect the ENDOR line. Furthermore, a temperature increase should decrease E when $\tau^{-1} > \omega$, should leave E nearly unchanged when $\tau^{-1} = \omega$, and should increase E when $\tau^{-1} < \omega$. These three effects have all been observed in the present study, in that order with photopolymerized VMA, DMA, and TMA. This means that the methyl group rotates more freely in VMA (less cross-linked polymer) than in the other two, more cross-linked polymeric systems. Furthermore, the fact that temperature does not significantly change τ^{-1} in the case of DMA suggests that, in this case, τ^{-1} must be very close to the value at which E is maximum, *i.e.* to $1/\omega = 2 \times 10^4$ ps, a value very similar to the above cited one for irradiated (−)-alanine.

On the other hand, in all the systems examined here (photopolymerized VMA, DMA and TMA) further cross-linking produced in the polymeric structure on heating of the samples at 393 K for 1 h probably reduces the methyl rotation speed to such a low value that the modulation of the hfcc of the methyl group is no more an effective source of relaxation to produce ENDOR enhancement, and the ENDOR band due to the methyl group irreversibly disappears. However, we must also mention that after this thermal treatment two new EPR lines appeared in the EPR spectrum of pre-irradiated TMA (see Fig. 3) and DMA,[14] suggesting that some deeper transformation leading to radical species other than the propagation radical could have occurred in the sample.

Dispersive kinetics of radical decay

Radical decay is accompanied by an increase in the fraction of S• radicals undergoing spin–spin exchange, as shown in Fig. 4. Radicals S• can only be generated from radicals R•, in a monomolecular or a bimolecular step. The kinetic picture is further complicated by the fact that the concentration of the radical species giving the two extra EPR lines (Fig. 2) at high temperature in pre-irradiated DMA and TMA cannot be estimated through the fitting procedure.

In an attempt to rationalize the experimental results of radical decay in a quantitative manner, we verified that the integrated area of the nine-line EPR pattern decreases according to a bimolecular process, as expected from the classical termination mechanism. Linear plots of the reciprocal radical R• concentration *vs.* time have been obtained at 423 K for all photopolymerized methacrylates (VMA, TMA and DMA), while a decrease in slope of these plots (*i.e.* in rate constant) with increasing time has been observed at lower temperatures. Thus, termination due to the R• + S• encounter, *i.e.* involving radical species trapped in different polymeric phases, seems less probable, as already observed in similar cases,[13] than does an R• + R• interaction leading to radical termination or production of S• species. The former interaction would simply cause the exchange process of eqn. (2).

The observed decrease in bimolecular rate constant during radical decay kinetics, which is accompanied by further polymerization and cross-linking, can be easily explained by considering that radicals are trapped in a solid glassy matrix. They can migrate and encounter other radicals only through chain propagation or chain transfer, and not through free diffusion, as in gas or liquid phases. The laws of classical kinetics in fluid systems do not apply any more in these conditions and much effort has been spent in recent years in order to model the process, through statistical,[22–24] kinetically based[25,26] or structure simulation[27–29] approaches. We found that our radical decay results can be satisfactorily interpreted in the light of a dispersive kinetic model.[24]

The dispersive nature of kinetics becomes evident in solids when the rates of reactions approach those of structural relaxation, and in the limit case the reaction patterns follow from reaction modelling in statistically disordered systems. Within this framework, the reaction rate constant k of classical kinetics is replaced by the time-dependent specific reaction rate $k(t)$ given in eqn. (4), where B is a constant, while the parameter

$$k(t) = Bt^{\alpha - 1}, \qquad 0 < \alpha \leq 1 \qquad (4)$$

α measures the dispersion of activation energy of the reaction.[30] For $\alpha \rightarrow 1$, the rate coefficient k is no longer time dependent and a classical kinetic law applies. In the case of second-order kinetics the integrated rate equation with the time-dependent rate coefficient $k(t)$ is given by eqn. (5) where [R•] and $[R^{\bullet}]_0$ are the concentrations of radical R• at time t and at the beginning of radical decay, respectively.

Table 2 Rate (B) and dispersion (α) parameters calculated from eqn. (5) for radical R$^{\bullet}$ decay in methacrylate monomers pre-irradiated in the presence of 1.0 wt.% photoinitiator

Monomer	T/K	$[R^{\bullet}]_0$[a]/mol dm^{-3}	α	B[a]/dm^3 mol^{-1} min$^{-\alpha}$
DMA	363	6.1×10^{-3}	0.43 ± 0.05	1.0
DMA	393	5.4×10^{-3}	0.93 ± 0.01	1.2
DMA	423	3.8×10^{-3}	1.00 ± 0.01	13
DMA + TMA[b]	393	1.7×10^{-3}	0.81 ± 0.04	2.7
TMA	363	2.0×10^{-3}	0.38 ± 0.02	2.8
TMA	393	8.6×10^{-4}	0.56 ± 0.02	18
TMA	423	6.9×10^{-4}	1.00 ± 0.03	36
VMA	363	3.1×10^{-4}	0.63 ± 0.03	8.4
VMA	393	2.3×10^{-4}	0.79 ± 0.03	190
VMA	423	7.2×10^{-4}	0.96 ± 0.08	1200

[a] Absolute values are rough estimates. [b] A 50/50 wt.% mixture of the two monomers.

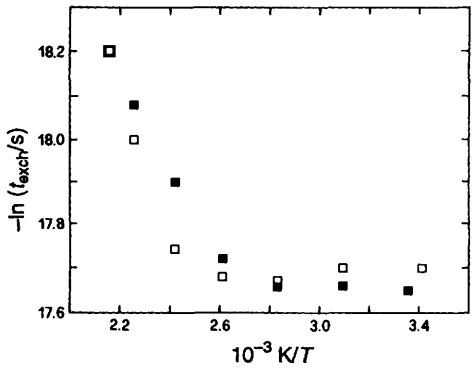

Fig. 9 Plot of $-\ln(t_{exch}/s)$ *vs.* reciprocal temperature for photopolymerized (■) TMA and (□) VMA

$$[R^{\bullet}]^{-1} - [R^{\bullet}]_0^{-1} = \frac{B}{\alpha} t^{\alpha} \qquad (5)$$

The fitting of our experimental data according to eqn. (5) gave very good correlations. The B and α parameters calculated by this way are reported in Table 2. α-Values increase with temperature, being rather low at 363 K and somewhat higher, but in any case lower than 1, at 393 K, thus confirming the dispersive nature of radical decay kinetics in this temperature range. In contrast, $\alpha \cong 1$ in all cases at 423 K, suggesting that radical decay occurs according to a classical bimolecular termination mechanism at temperatures above the glass transition of the polymeric systems (*e.g.*, ~413 K for photopolymerized DMA[31]). B-Values are sensitive to the conversion degree of methacrylate groups which had been reached by irradiation in each polymeric system, and increase with temperature, as expected. Radicals R$^{\bullet}$ decay at the fastest rate in photopolymerized VMA, which consequently should be the system in which polymeric chains maintain the highest mobility. However, according to eqn. (4), both α and B parameters determine the effective rate of radical decay. In the case of radical decay in a photopolymerized mixture of TMA and DMA at 393 K (see also Fig. 5) both parameters have intermediate values with respect to those determined for the two photopolymerized monomers at the same temperature. Dispersive kinetics is thus a very good model for the quantitative interpretation of radical decay results in glassy polymers, leading to evaluation of parameters which well characterize the polymeric structure.

The dependence of the dynamic exchange process between two radical conformations $R_1^{\bullet}$ and $R_2^{\bullet}$ on temperature further supports the validity of the dispersive kinetic model applied to the characterization of polymeric structures. The rate of exchange t^{-1}_{exch} (Fig. 9) does not increase with temperature according to a simple Arrhenius plot, as the exchange activation energy increases continuously with increasing temperature. This trend is perfectly compatible with the behaviour expected from the dispersive kinetic model, which predicts noticeable variations in activation energy around the transition temperature T_g of the polymer, as very recently reported.[32] If the temperature is below T_g, in fact, the activation energy E approaches the activation energy value E_ζ which is expected for the process under analysis (exchange between two conformations, in the present case). In polymers E_ζ is up to two orders of magnitude lower than the configurational activation energy E_{τ_0}, due to polymer matrix structural relaxation. On the other hand, at the high temperature limit eqn. (6) holds, *i.e.*,

$$E = \alpha E_\zeta + (1 - \alpha) E_{\tau_0} \qquad (6)$$

activation energies are higher because they include the contribution $(1 - \alpha)$ times the activation energy E_{τ_0} for matrix structural relaxation. The results illustrated in Fig. 9 indicate that the activation energy of radical conformation exchange in both photopolymerized TMA and VMA is very low at relatively low temperatures, while it increases with increasing temperature, tending to a much higher, constant value. The observed trend confirms that pre-irradiated VMA should maintain a higher segmental mobility than pre-irradiated TMA, having a lower T_g-value.

Acknowledgements

This work was financially supported by the Ministero dell'Università e della Ricerca Scientifica e Tecnologica. We thank Dr M. Barzaghi for helpful discussions.

References

1 B. C. Gilbert, J. R. Lindsay Smith, E. C. Milne, A. C. Whitwood and P. Taylor, *J. Chem. Soc., Perkin Trans. 2*, 1994, 1759.
2 B. Rånby and J. F. Rabek, *ESR Spectroscopy in Polymer Research*, Springer Verlag, Berlin, 1977.
3 E. Selli and I. R. Bellobono, in: *Radiation Curing in Polymer Science and Technology*, ed. J.-P. Fouassier and J. F. Rabek, Elsevier, London, 1993, vol. 3, ch. 1.
4 G. R. Tryson and A. R. Shultz, *J. Polym. Sci., Polym. Phys. Ed.*, 1979, **17**, 2059.
5 J. G. Kloosterboer, *Adv. Polym. Sci.*, 1988, **84**, 1.
6 C. Decker and K. Moussa, *Eur. Polym. J.*, 1990, **26**, 393.
7 M. Buback, R. G. Gilbert, G. T. Russell, D. J. Hill, G. Moad, K. F. O'Driscoll, J. Shen and M. A. Winnik, *J. Polym. Sci., Polym. Chem. Ed.*, 1992, **30**, 851.
8 J. G. Kloosterboer, G. M. M. van de Hei and H. M. J. Boots, *Polym. Commun.*, 1984, **25**, 354.
9 M. P. Tonge, R. J. Pace and R. G. Gilbert, *Macromol. Chem. Phys.*, 1994, **195**, 3159.
10 I. R. Bellobono, C. Oliva, R. Morelli, E. Selli and A. Ponti, *J. Chem. Soc., Faraday Trans.*, 1990, **86**, 3273.

11 C. Oliva, E. Selli, A. Ponti, I. R. Bellobono and R. Morelli, *J. Phys. Org. Chem.*, 1992, **5**, 55.
12 E. Selli, C. Oliva, M. Galbiati and I. R. Bellobono, *J. Chem. Soc., Perkin Trans. 2*, 1992, 1391.
13 E. Selli, C. Oliva and A. Giussani, *J. Chem. Soc., Faraday Trans.*, 1993, **89**, 4215.
14 E. Selli, C. Oliva and G. Termignone, *J. Chem. Soc., Faraday Trans.*, 1994, **90**, 1967.
15 B. Chu and D. Lee, *Macromolecules*, 1984, **17**, 926.
16 M. Barzaghi and M. Simonetta, *J. Magn. Reson.*, 1983, **51**, 175.
17 M. Kamachi, Y. Kuwae, M. Kohno and S. Nazakura, *Polym. J.*, 1985, **17**, 541.
18 D. S. Leniart, J. S. Hyde and J. C. Vedrine, *J. Phys. Chem.*, 1972, **76**, 2079.
19 N. M. Atherton, *Principles of Electron Spin Resonance*, Ellis Horwood, London, 1993, ch. 9.
20 M. Brustolon, T. Cassol, L. Micheletti and U. Segre, *Mol. Phys.*, 1986, **57**, 1005.
21 M. Brustolon, T. Cassol, L. Micheletti and U. Segre, *Mol. Phys.*, 1987, **61**, 249.
22 C. W. Macosko and D. R. Miller, *Macromolecules*, 1976, **9**, 199.
23 A. B. Scranton and N. A. Peppas, *J. Polym. Sci, Part A: Polym. Chem.*, 1990, **28**, 39.
24 A. Plonka and A. Paszkiewicz, *J. Chem. Phys.*, 1992, **96**, 1128.
25 A. G. Mikos, C. G. Takoudis and N. A. Peppas, *Polymer*, 1987, **28**, 998.
26 H. Tobita and A. E. Hamielec, *Macromolecules*, 1989, **22**, 3098.
27 H. M. J. Boots and R. B. Pandey, *Polym. Bull.*, 1984, **11**, 415.
28 G. P. Simon, P. E. M. Allen, D. J. Bennett, D. R. G. Williams and E. H. Williams, *Macromolecules*, 1989, **22**, 3555.
29 K. S. Anseth and C. N. Bowman, *Chem. Eng. Sci.*, 1994, **49**, 2207.
30 A. Plonka, *Radiat. Phys. Chem.*, 1991, **37**, 555.
31 D. Li, S. Zhu and A. E. Hamielec, *Polymer*, 1993, **34**, 1383.
32 A. Plonka, *Radiat. Phys. Chem.*, 1995, **45**, 67.

Paper 5/02074C
Received 31*st March* 1995
Accepted 23*rd June* 1995